Published in final edited form as:
Cancer Res. 2011 October 15; 71(20): 6371–6381. doi:10.1158/0008-5472.CAN-11-0991.

Glioblastoma angiogenesis and tumor cell invasiveness are differentially regulated by β8 integrin

Jeremy H. Tchaicha[*,†], **Steve B. Reyes**[*], **Jaekyung Shin**[¥], **Mohammad G. Hossain**[*], **Frederick F. Lang**[#], and **Joseph H. McCarty**[*,Ω]

[*]Department of Cancer Biology, University of Texas M.D. Anderson Cancer Center

[¥]Department of Biochemistry and Molecular Biology, University of Texas M.D. Anderson Cancer Center

[#]Department of Neurosurgery, University of Texas M.D. Anderson Cancer Center

Abstract

Glioblastoma multiforme (GBM) is a highly invasive brain tumor that develops florid microvascular proliferation and hemorrhage. However, mechanisms that favor invasion versus angiogenesis in this setting remain largely uncharacterized. Here we show that integrin β8 is an essential regulator of both GBM-induced angiogenesis and tumor cell invasiveness. Highly angiogenic and poorly invasive tumors expressed low levels of β8 integrin, whereas highly invasive tumors with limited neovascularization expressed high levels of β8 integrin. Manipulating β8 integrin protein levels altered the angiogenic and invasive growth properties of GBMs, in part reflected by a diminished activation of latent transforming growth factor βs (TGFβs), which are extracellular matrix (ECM) protein ligands for β8 integrin. Taken together, these results establish a role for β8 integrin in differential control of angiogenesis versus tumor cell invasion in GBM. Our findings suggest that inhibiting β8 integrin or TGFβ signaling may diminish tumor cell invasiveness during malignant progression and following anti-vascular therapies.

Keywords

extracellular matrix; astrocyte; astrocytoma; cell adhesion; TGFβ

Introduction

Astrocytomas, which arise from presumptive astrocytes and/or neural progenitor cells of origin (1), afflict approximately 20,000 people within the United States each year (2). They represent the most common type of primary brain tumor, and in their malignant stages they are one of the deadliest forms of cancer. Multiple chromosomal abnormalities and gene expression defects correlate with astrocytoma initiation and progression (3). For example, low grade astrocytomas commonly display loss of p53, and as these tumors progress to more malignant stages they often show deletion of the Ink4/Arf tumor suppressors (4). Grade IV astrocytomas, or GBMs, commonly display amplification of PDGF-B and/or EGF receptor expression, leading to hyperactivation of downstream signaling cascades often involving Ras (5).

[Ω]Corresponding author: Joseph H. McCarty Department of Cancer Biology, Unit 173 M.D. Anderson Cancer Center 1515 Holcombe Boulevard Houston, TX 77030 jhmccarty@mdanderson.org.
[†]Current address: Dana Farber Cancer Institute, 44 Binney St., Boston, MA

GBMs develop unique angiogenesis pathologies including microvascular hyperproliferation well as edema and hemorrhage owing to breakdown of the intratumoral blood-brain barrier (6). GBM cells are also highly infiltrative, often dispersing to distal regions of the brain via white matter tracts and vascular basement membranes (7, 8). GBM-induced angiogenesis and tumor cell invasiveness are tightly coupled pathologies. For example, anti-vascular therapies commonly enhance perivascular GBM cell invasiveness, leading to the development of secondary lesions that are resistant to second-line therapies (9, 10).

GBM-induced angiogenesis and tumor cell invasion are influenced by a milieu of growth factors and extracellular matrix (ECM) cues within the brain microenvironment (6). Most mammalian cells communicate with protein components in the ECM via a family of cell surface receptors known as integrins (11). The five members of the αv integrin subfamily- αvβ1, αvβ3, αvβ5, αvβ6 and αvβ8- are expressed in neural and vascular cells of the brain and bind to RGD peptide motifs present in many shared ECM ligands (12). In particular, genetic studies in mice have revealed that αvβ8 integrin is a central regulator of angiogenesis in the developing brain (13, 14). Targeted ablation of αv or β8 integrin genes in embryonic neuroepithelial cells causes brain-specific vascular phenotypes, including endothelial cell hyperproliferation, the formation of vessels with glomeruloid-like tufts, and intracerebral hemorrhage (15, 16). These pathologies are due to defective activation of latent TGFβs, which are ECM-bound protein ligands for αvβ8 integrin (17, 18). In neurogenic regions of the adult mouse brain αvβ8 integrin is expressed in neural stem and progenitor cells where it governs proper neurogenesis (19) and neuroblast migration (20).

αvβ8 integrin expression and functions are dysregulated in various brain pathologies. For example, diminished expression of αvβ8 integrin and reduced TGFβ signaling are detected in brain arteriovenous malformations (21). We have discovered that αvβ8 integrin-activated TGFβs suppress pathological angiogenesis in mosaic mouse models of astrocytoma (22). Here, we have analyzed roles for αvβ8 integrin in angiogenesis and tumor cell invasiveness in human GBM. Using xenograft models as well as cell culture systems we demonstrate that β8 integrin differentially regulates these GBM pathologies, in part, via autocrine activation of TGFβ signaling pathways.

Materials and Methods

GBM cell lines and human tumor samples

Approval for the use of human specimens was obtained from the Institutional Review Board (IRB) at The University of Texas M. D. Anderson Cancer Center. The IRB waived the requirement for informed consent for previously collected residual tissues from surgical procedures stripped of unique patient identifiers according to Declaration of Helsinki guidelines. LNZ208 and LN428 cells were provided by Dr. Oliver Bogler (MD Anderson Cancer Center) and were authenticated by short tandem repeat analysis in 2009. U87, LN18, LN229, SNB19, and U373 GBM cell lines were purchased from ATCC (Manassas, VA). Short tandem repeat analyses by ATCC have revealed that SNB19 and U373 are from the same patient. All cells were grown in DMEM/F12 (Mediatech) supplemented with 10% fetal bovine serum (Atlanta Biologics) and antibiotics. Normal human astrocytes were purchased from Lonza, Inc. Transformed human astrocytes (THAs) have been described elsewhere (23). β8 integrin protein was overexpressed in U87 cells using a pcDNA4.0 plasmid harboring a full-length human β8 integrin cDNA fused at the C-terminus with a V5 epitope tag. After selection for 10 days in 300 μg/ml zeocin stable transfectants were pooled and analyzed.

Antibodies

The following antibodies were purchased from commercial sources: rat anti-mouse CD34 mAb (Genetex), rat anti-mouse CD31 (Pharmingen), rabbit anti-α-actin (Sigma) and mouse anti-human αv integrin mAb (BD Biosciences). FITC-conjugated phalloidin was purchased from Sigma. The anti-αv integrin and anti-β8 integrin rabbit polyclonal antibodies used for immunoblotting have been described elsewhere (24, 25). Secondary antibodies were goat anti-rabbit, goat anti-chicken, goat anti-rat and goat anti-mouse, all conjugated to Alexa488 or Alexa594 (Molecular Probes). HRP-conjugated secondary antibodies used were sheep anti-mouse, goat anti-rabbit and donkey anti-chicken IgY (Jackson ImmunoResearch Labs). NIH ImageJ software was used for quantitation of intratumoral blood vessel densities based on anti-CD34 fluorescence intensity.

To generate the anti-β8 integrin antibody used for GBM immunohistochemistry a 43-kDa fragment of the β8 integrin extracellular domain (β8ex) was expressed in bacteria as a GST fusion protein using the pGEX-6P expression plasmid (GE Healthcare). The DNA primer sequences used to amplify the β8ex region are: 5'-TCAGTTGATTCAATAGAATACC-3' and 5'-CTGTGTATATGAATTTTAGCG-3'. GST-β8ex protein (~67 kDa) was found exclusively in detergent-insoluble inclusion bodies. GST-β8ex was solubilized in buffer containing 6M urea and sequentially dialyzed into urea-free buffer. Soluble recombinant protein was fractionated using glutathione-Agarose. The GST portion was cleaved using Precision Protease (GE Healthcare) to liberate the 43-kDa β8ex protein, which was used to immunize rabbits (Covance).

Immunohistochemistry and immunofluorescence

Formalin fixed paraffin embedded (FFPE) sections were deparaffinized in 2 changes of xylene and then dehydrated in 2 changes of 100% ethanol, 95% and 80% ethanol, and distilled water. For anti-αv integrin immunohistochemistry, slides were incubated 95-100°C with pH 9.0 antigen retrieval buffer (DAKO) for 40 minutes and then transferred to room temperature prior to immunostaining. Alternatively, deparaffinized sections were incubated in blocking solution and then primary anti-β8ex antibody was added. Sections were rinsed three times with PBS, blocked with peroxidase solution, incubated with secondary antibodies conjugated to HRP, and then VIP or DAB chromagens were added to visualize immunoreactivity. For quantitation of blood vessel densities in tumors generated from U87 cells and THAs, digital images were selected from three intratumoral regions labeled with anti-CD34 antibodies. Three serial sections were analyzed from 3 different mice injected with the various cell types. Mean fluorescence intensity was calculated using NIH ImageJ software. Two investigators, who were blinded to the identities of each sample, analyzed sections.

Generation of lentivirus-expressing shRNAs

For lentiviral-mediated silencing DNA the following synthetic oligonucleotides were used: 5'-TGTATCCTCATCATGATGTGTTCAAGAGACACATCATGATGAGGATACTTTTTTC-3', and 5'-TCGAGAAAAAAGTATCCTCATCATGATGTGTCTCTTGAACACATCATGATGAGGATACA-3'. The oligonucleotides were ligated into the pLB lentiviral gene-transfer vector (26) using HpaI and XhoI restriction sites. This pLB vector contains a U6 promoter that drives expression of shRNAs, and a CMV promoter driving GFP expression. Packaged lentiviruses were generated by transfecting HEK 293-FT cells (ATCC) with pLB transfer vectors in combination with plasmids encoding gag/pol and VSV-G envelope proteins.

Stereotactic injections

All animal procedures were conducted under IACUC-approved protocols. NCR-nu/nu male mice (Jackson Laboratories) were anesthetized and a single incision was made from the anterior pole of the skull to the posterior ridge. We targeted the striatum for cell implantation using the following stereotactic coordinates: 1.5 mm rostral, 1.5 mm anterior, and 4 mm below the pial surface. An automated micropump (Stoelting Instruments) was used to dispense cells in 3 μl PBS over a five-minute period. To generate intracranial tumors from THAs, we injected 2.5×10^5 cells for analysis of tumor-induced angiogenesis, tumor cell invasiveness, and tumor volumes. Kaplan-Meier survival analysis was performed after injecting 5×10^4 THAs per mouse. Human intracranial xenograft tumors were generated by injecting 5×10^5 U87 or SNB19 cells into the striatum of NCR-nu/nu mice. Animals were monitored for tumor-induced neurological deficits and moribund animals were euthanized with gaseous CO_2. Mice were perfused with 4% PFA/PBS and brains were coronally sliced at 1 mm intervals and paraffin-embedded tissues were serially sectioned at 7 μm intervals.

PAI1-Luciferase assays

THAs were transiently transfected with a PAI1-Luciferase plasmid (27). 4×10^5 cells were seeded onto 6-well plates coated with poly-D-lysine (Sigma), and four hours later media was removed and serum-free media was added for 24 hours. Cell lysates were prepared and firefly luciferase activities were quantified (Enhanced Luciferase Assay Kit, BD Biosciences).

Invasion and Migration Assays

5×10^4 THAs were added in serum-free media to the upper chambers of matrigel invasion transwell systems (BD Biosciences, 8 μm pore sizes). Normal growth medium containing 10% FBS was added to the lower wells and invasion was quantified after 18 hours by staining the transwell filters with crystal violet. Alternatively, THAs were plated onto laminin-coated coverslips in 24 well dishes (1×10^5 cells/well). After reaching confluence cells were wounded with a 10 μl pipette tip. Cell migration was analyzed at various time points by fixing cells and labeling with phalloidin-FITC or anti-paxillin antibodies. Alternatively, migration was imaged by time-lapse microscopy using an Olympus IX81 inverted microscope mounted with an automated stage, humidified chamber and DP25 digital camera. SlideBook software (Intelligent Imaging Innovations) was used to quantify migration. Migration was analyzed in separate frames and wound closure was defined when five migrating cells from opposite sides of the scratch (within a 200x field) made contacts within the wound region.

Alternatively, siRNA pools (Dharmacon) targeting human β8 integrin were transfected into LN229 GBM cells using manufacturer-supplied transfection reagents and protocols. 48 hours after transfection cells were either lysed to confirm integrin silencing by immunoblotting, or analyzed in the matrigel invasion system using 5×10^4 cells per transwell as detailed above.

Statistical Analyses

Student's t-test was performed to determine statistically significant differences between groups. The Wilcoxan Rank Sum Test was used for analysis of Kaplan-Meier survival results. Microsoft excel was used to calculate statistics.

Results

Analysis of β8 integrin protein expression patterns in human GBM cell lines in vitro and GBMs in situ

We used anti-β8 integrin and anti-αv integrin antibodies to screen normal human astrocytes (NHAs), transformed human astrocytes (THAs), and 7 different human GBM cell lines for levels of integrin protein expression. As shown in Figure 1A, all cell types expressed similar levels of αv integrin protein, whereas β8 integrin protein was expressed at varying levels in the different cell types. NHAs expressed robust levels of β8 integrin and oncogene-mediated transformation of these cells resulted in a significant reduction in integrin protein expression. The human GBM cell lines U373, LNZ208, LN428, SNB19 and LN229 cells all expressed robust levels of β8 integrin protein. In contrast, U87 and LN18 cells expressed low or undetectable levels of β8 integrin protein (Figure 1A). Plasma membrane expression of αvβ8 integrin protein was confirmed using a membrane-impermeable reactive biotin derivative to label cells. Detergent-soluble lysates were then immunoprecipitated using anti-αv and anti-β8 integrin antibodies to reveal cell surface expression (Supplemental Figure 1).

We also compared integrin expression levels by immunoblotting lysates prepared from 7 different freshly resected GBM samples. All samples expressed similar levels of αv integrin protein, and 6 of the 7 samples expressed robust levels of β8 integrin protein with one sample expressing lower levels of β8 integrin (Figure 1B). Robust levels of αvβ8 integrin protein were also detected in lysates prepared from three freshly resected grade III anaplastic astrocytomas, two grade IV oligodendrogliomas, and one gliosarcoma (data not shown).

The anti-β8 integrin antibody used for immunoblotting (Figures 1A, B) was not compatible for immunohistochemical labeling of formalin fixed paraffin embedded (FFPE) tumor sections. Therefore, we generated polyclonal antisera directed against the extracellular portion of human β8 integrin. The antiserum is highly specific for human β8 integrin protein and shows minimal cross-reactivity with mouse β8 integrin (Supplemental Figures 2 and 3). FFPE samples corresponding to three of the 7 GBM samples analyzed in Figure 1B were analyzed by anti-αv and anti-β8 integrin immunohistochemistry. As shown in Figures 1C, a commercially available anti-αv mAb revealed integrin protein expression in intratumoral blood vessels as well as in GBM cells. The immunoreactivity was likely due to αvβ3 integrin, which is expressed in vascular endothelial cells of GBMs and other malignant neural tumors (28, 29). We detected β8 integrin protein expression in most GBM cells (Figure 1C); however, little if any β8 integrin protein was detected in the intratumoral vasculature. These data are consistent with a prior report showing β8 integrin mRNA and protein expression in human GBM cells but not blood vessels (30). These immunohistochemical results confirm our analyses of αv and β8 integrin protein expression in lysates prepared from normal human astrocytes, GBM cell lines, and GBMs (Figures 1A, B).

Exogenous expression of β8 integrin in U87 GBM cells leads to diminished intratumoral vascular pathologies

To analyze β8 integrin functions in GBMs in vivo, we forcibly expressed V5-tagged human β8 integrin protein in U87 GBM cells, which express low levels of endogenous β8 integrin (Figure 1A). In comparison to control U87 cells transfected with empty vector, increased β8 integrin protein expression was detected in pools of cells stably overexpressing β8-V5 integrin (Figure 2A). Next, stably transfected control cells or U87 cells overexpressing β8-V5 protein were injected into the brains of NCR-nu/nu mice (n=5 mice per genotype). After 4 to 6 weeks mice were sacrificed, cardiac-perfused with fixative, and brains were slice coronally to analyze integrin-dependent differences in tumorigenicity. As shown in Figure

2B, U87 cells stably transfected with empty plasmid and U87 cells stably expressing β8-V5 integrin both generated large intracranial tumors. Tumors generated from control U87 cells lacking β8 integrin expression, however, showed grossly obvious hemorrhage and edema. In contrast, U87 tumors expressing β8-V5 protein were vascularized but did not contain severe hemorrhage and edema. Intratumoral blood vessel densities were quantified by immunolabeling U87 tumor sections with anti-CD34 antibodies (n=3 different tumors per cell type, n=3 sections per tumor). As shown in Figure 2C, we detected distended, sinusoidal-like vessels throughout GBMs generated from U87 cells stably transfected with empty plasmids. U87 cells stably overexpressing β8-V5 protein also yielded well-vascularized tumors; however, the abnormal blood vessel morphologies were not evident with most vessels displaying small, capillary-like morphologies. In addition, intratumoral vascular densities, based on quantitation of CD34 fluorescence, were diminished significantly in U87 tumors overexpressing β8 integrin protein (Figure 2D).

RNAi-mediated silencing of β8 integrin gene expression impacts angiogenesis and tumor cell invasiveness in human GBMs

We selected LN229 and SNB19 GBM cell lines that expressed high levels of endogenous β8 integrin protein (Figure 1A), and attempted to stably silence integrin expression using lentiviral-delivered shRNAs. These efforts resulted in only ~60% reduction in β8 integrin protein expression in pools of stably transfected cells (data not shown). Analysis of in vitro and in vivo growth and invasive properties in LN229 and SNB19 cells expressing diminished β8 integrin protein, however, did not reveal obvious differences in comparison to control cells (data not shown). Our prior studies of cultured astrocytes and neural progenitors from β8+/- mice, which express 50% less β8 integrin protein in comparison to wild type controls, revealed no differences in cell behaviors (data not shown), suggesting that nearly complete silencing of integrin expression is likely required to reveal functional roles in cells. Therefore, we stably silenced β8 integrin expression in transformed human astrocytes (THAs), which express lower levels of β8 integrin protein (Figure 1A) and represent a more genetically tractable model system for in vitro and in vivo studies. THAs were generated by infecting NHAs with retroviruses engineered to express human papilloma virus E6 and E7 proteins, oncogenic H-Ras (^{G12V}H-Ras) and hTERT (23). E6/E7 oncoproteins inhibit the expression and function of the p53 and Rb tumor suppressors, respectively. p53 is commonly mutated or deleted in human GBMs, and both p53 and Rb negatively regulate the functions of the Ink4a/Arf tumor suppressors, which are also commonly deleted in malignant GBMs (31, 32). Ras activities are often hyperactivated in GBMs, owing to gene mutations or elevated expression of EGF receptors (33), and hTERT overexpression is necessary for maintaining telomeres in human cancer cells (34).

THAs were stably transduced with either scrambled shRNAs (controls) or two different shRNAs targeting β8 integrin and cells were fractionated based on GFP expression (Supplemental Figures 4A, B). Integrin gene silencing was confirmed by immunoblotting detergent-soluble lysates (Figure 3A) or immunoprecipitating integrins from biotinylated cell lysates using anti-αv and anti-β8 antibodies (Figure 3B). Both shRNAs significantly reduced β8 integrin expression, although one was used to analyze THA behaviors in vitro and in vivo. In comparison to THAs expressing scrambled shRNAs, cells expressing β8 shRNAs produced significantly more colonies in three-dimensional soft agar assays (Supplemental Figure 4C). We next analyzed β8 integrin-dependent effects on tumor growth, angiogenesis and tumor cell invasiveness in vivo. THAs expressing scrambled shRNAs or β8 shRNAs were stereotactically injected in the striatum of immune-compromised mice (n=5 mice/cell type, 2.5×10^4 cells/mouse). Within 5 to 6 weeks after injection all mice developed obvious signs of tumor burden including weight loss and neurological deficits such as ataxia. Nearly all mice (n=4 of 5 animals) injected with THAs

expressing β8 shRNAs also developed severe hydrocephaly (data not shown). Gross analysis of intracranial tumors derived from THAs expressing control shRNAs reveal localized lesions adjacent to the lateral ventricles; in contrast, astrocytomas formed from THAs expressing diminished β8 integrin protein were significantly larger, and showed severe edema and hemorrhage (Figure 3C). Quantitation of tumor volumes in H&E stained histological sections revealed that astrocytomas expressing β8 shRNAs were significantly larger (Figure 3D, left panel). Kaplan-Meier survival comparisons revealed that mice harboring astrocytomas expressing β8 shRNAs died significantly earlier (Figure 3D, right panel), likely due to larger tumor sizes and associated neurological deficits.

Coronal sections were H&E-stained to reveal that THAs expressing control shRNAs were well vascularized, with intratumoral endothelial cells expressing laminin (Figure 4A, left panels). Astrocytomas expressing β8 shRNAs contained obvious abnormalities in blood vessel morphologies as revealed by H&E and anti-laminin staining (Figure 4A, right panels), with many vessel displaying distended, sinusoidal-like morphologies. Quantitation of intratumoral blood vessels by anti-CD34 immunofluorescence and quantitation using ImageJ software revealed significantly higher numbers of vessels in astrocytomas expressing β8 shRNAs (Figure 4B). Astrocytomas expressing scrambled shRNAs grew in periventricular regions of the brain and were infiltrative, with invading astrocytoma cells detected several microns from the main tumor mass (Figure 4C, left panels). In contrast, THAs expressing β8 shRNAs generated larger, noninfiltrative astrocytomas. Dissemination of GFP-expressing tumors cells into the surrounding brain parenchyma was not detected in the absence of β8 integrin expression (Figure 4C, right panels). Invasion assays through three-dimensional ECM were also used to quantify integrin-dependent THA invasion. As shown in Figure 4D, in comparison to THAs expressing scrambled shRNAs, cells expressing β8 shRNAs showed a significant decrease in invasiveness. This integrin-dependent defect in cell invasion was not specific for THAs, since LN229 human GBM cells, which express robust levels of β8 integrin (Figure 1A), showed a significant reduction in invasiveness following transient siRNA-mediated silencing of β8 integrin expression (Supplemental Figure 5).

Hypoxia within the tumor microenvironment has been reported to influence GBM cell growth and invasiveness; for example, mouse astrocytoma cells genetically null for hypoxia inducible factor 1 α (Hif1α) or the Hif1α-inducible gene, VEGF-A, show highly invasive intracranial growth patterns (35). To address potential functional links between hypoxia and αvβ8 integrin-mediated astrocytoma cell invasiveness, Hif1α protein levels were interrogated in astrocytomas derived from control THAs or THAs manipulated to express diminished levels of β8 integrin (n=3 tumors per cell type, n=3 sections per tumor). In comparison to tumors expressing control shRNAs (Supplemental Figure 6A), we detected elevated levels of Hif1α protein in tumors expressing β8 shRNAs (Supplemental Figure 6B). Integrin-dependent increases in Hif1α protein expression were not detected in vitro (Supplemental Figure 6C). We detected an approximately 50% reduction in VEGF-A protein in THAs expressing β8 shRNAs (Supplemental Figure 6D), although integrin-dependent differences in VEGF-A protein expression in astrocytoma sections were not evident (data not shown). Taken together, these data suggest that β8 integrin is interconnected with the Hif1α/VEGF-A signaling cascade, and these events drive astrocytoma cell invasiveness.

β8 integrin-mediated TGFβ activation and signaling are essential for astrocytoma cell polarity and directional migration—In the developing brain β8 integrin is a receptor for ECM-bound latent TGFβs, and mediates their activation and subsequent receptor engagement (36). To investigate roles for αvβ8 integrin-mediated TGFβ activation in astrocytoma cells, THAs expressing scrambled shRNAs or β8 shRNAs were

transiently transfected with a reporter plasmid consisting of the TGFβ-responsive PAI1 promoter driving expression of firefly luciferase (27). Levels of firefly luciferase activity were analyzed after 24 hours. As shown in Figure 5A, approximately four-fold less luciferase activities were detected in THAs expressing β8 shRNAs, reflecting diminished endogenous β8 integrin-mediated TGFβ activation and signaling. These results showing β8 integrin is a mediator of latent TGFβ1 activation and signaling in astrocytoma cells are consistent with our prior data revealing that neural stem and progenitor cells also utilize β8 integrin to activate latent TGFβs to control cell growth and differentiation in neurogenic regions of the mouse brain (19).

Astrocytoma cell polarity and directional migration were next analyzed using in vitro scratch-wound assays (37). Confluent monolayers of THAs expressing scrambled shRNAs or β8 shRNAs (n=3 different samples per cell type) were wounded using a pipet tip. After two hours polarity was monitored by labeling cells with phalloidin or anti-paxillin antibodies to visualize the actin cytoskeletal network and cell-ECM contacts, respectively. THAs expressing control shRNAs displayed paxillin-positive adhesion sites at the leading edge (Supplemental Figure 7A), whereas THAs expressing β8 shRNAs displayed fewer paxillin-containing focal adhesion complexes at their leading edges (Supplemental Figure 7B). THAs expressing scrambled shRNAs polarized in the direction of the wound and formed well-organized actin cytoskeletal networks (Supplemental Figure 7C); in contrast, THAs expressing β8 shRNAs showed diminished polarization at the wound edge, with few cells forming actin-rich projections into the wound region (Supplemental Figure 7D). Over a 24-hour period THAs expressing scrambled shRNAs largely filled the wound region, whereas migration by THAs expressing β8 shRNAs was significantly impaired as evidenced by failure to fill the wound area at 24 hours (Figure 5B).

TGFβs have been reported to promote cell migration in development and cancer (38, 39); therefore, we analyzed whether active TGFβs might enhance THA migration in vitro. As shown in Figure 5B, addition of 1 ng/ml of TGFβ1 enhanced directional migration in THAs expressing β8 shRNAs. To quantify roles for integrin-mediated TGFβ activation in THA migration, we imaged cell motility over 48 hours using time-lapse bright field microscopy (Supplemental Figure 7). THAs expressing scrambled shRNAs required approximately 24 hours to fill the wound regions, whereas THAs expressing β8 shRNAs required nearly 36 hours to fill the wound (Figure 5C). Exogenous addition of TGFβ1 showed a statistically significant rescue of the migration defects in THAs expressing β8 shRNAs (Figure 5C and Supplemental Figure 7). These data reveal that the β8 integrin-dependent astrocytoma cell polarity and migration defects are due, in part, to defective integrin-activated TGFβ signaling. These results also support our in vivo data showing diminished invasion by astrocytoma cells lacking β8 integrin (Figure 4), and support a model in which β8 integrin-mediated TGFβ activation is differentially involved in GBM neovascularization and tumor cell invasiveness (Figure 6).

Discussion

The data in this report reveal for the first time that αvβ8 integrin, via activation of its latent TGFβ protein ligands, plays central roles in regulating GBM-induced angiogenesis and perivascular tumor cell invasiveness. While various reports have shown elevated levels of TGFβ receptor signaling (40-42) in GBM cells, the factors that activate latent TGFβs within the tumor microenvironment remain obscure. Our data demonstrate that αvβ8 integrin is a positive regulator of the TGFβ signaling cascade in invasive GBM cells. We propose that distinct populations of GBM cells selectively express high versus low levels of αvβ8 integrin, with integrin protein expression levels directly determining tumor cell behaviors (Figure 6). While the exact mechanisms that regulate β8 integrin expression in GBM cells

remain obscure, a recent report has shown that β8 integrin is a direct target for miR-93, with mIR-mediated inhibition of β8 integrin expression correlating with enhanced angiogenesis and tumorigenicity (43). Therefore, it is enticing to speculate that during tumor growth and progression sub-populations of GBM cells selectively express high levels of miR-93, thus leading to diminished levels of β8 integrin and the development of angiogenesis pathologies. In contrast, we postulate that invasive GBM cells express low levels of mIR-93 and high levels of β8 integrin, leading to pro-invasive behaviors likely via autocrine activation of TGFβ signaling pathways. Interestingly, p38 and Sp-1 have also been reported to regulate β8 integrin gene expression (44), suggesting that genetic and epigenetic events may cooperatively control β8 integrin expression and functions in GBM-induced angiogenesis and tumor cell invasiveness.

Putative tumor suppressor-like roles for αvβ8 integrin have been reported in malignant cancers of the lung (45) and skin (46). Although adult β8-/- mice do not develop spontaneous brain tumors (19), we have found that THAs expressing diminished levels of β8 integrin form more colonies in vitro in soft agar assays and generate significantly larger astrocytomas in vivo, suggesting growth suppressive functions for this integrin. Tumor suppressor-like roles for integrin αvβ3 have been reported in mouse models of GBM. For example, in mouse astrocytoma cells αvβ3 integrin normally suppresses cell proliferation and genetic ablation of β3 integrin expression leads to enhanced tumorigenicity (47). However, human GBMs often display elevated levels of αvβ3 integrin, suggesting roles for this integrin in promoting tumor cell growth and/or invasion (48, 49). Indeed, small molecule inhibitors of αvβ3 cause diminished GBM cell growth and invasiveness *in vitro* and *in vivo* (50). αvβ3 integrin has been reported to activate focal adhesion kinase in cultured GBM cells (51) and inhibition of focal adhesion kinase activities leads to diminished GBM cell growth in vivo (52). It will be interesting to determine if αvβ8 integrin cooperatively signals with other integrins in GBM cells to regulate the activation of common intracellular effectors such as focal adhesion kinase.

Levels of hypoxia within the tumor microenvironment also influence GBM cell growth and invasiveness. For example, loss of Hif1α-inducible VEGF-A expression in mouse astrocytoma cells causes enhanced perivascular dispersal (35, 53). Interestingly, astrocytoma cells that express β8 shRNAs and are poorly invasive show elevated levels of Hif1α protein, although in these cells we detect reduced levels of VEGF-A (Supplemental Figure 6). Prior reports have shown that TGFβ-activated Smads function in concert with Hif1α to drive VEGF-A gene expression (54, 55), and THAs expressing β8 shRNAs show diminished TGFβ activation (Figure 5A). Therefore, we propose that these lower levels of VEGF-A expression are due in part to diminished integrin-activated TGFβ signaling, resulting in impaired functional links between Smads and Hif1α. Lastly, although our data point to critical roles in αvβ8 integrin-activated TGFβs in GBM-induced angiogenesis and tumor cell invasiveness in mouse models, these results require further corroboration in human GBM samples. It will be important to analyze levels of integrin protein expression and TGFβ signaling in invasive tumor cells in situ to determine the relative importance of this pathway in GBMs and other invasive human cancers.

Supplementary Material

Refer to Web version on PubMed Central for supplementary material.

Acknowledgments

We thank Dr. Russell Pieper (UCSF) for providing the transformed human astrocytes and Dr. Nami McCarty (UT-HSC) for helpful advice on lentivirus manipulations. This research was supported by grants awarded to J.H.M from

the Ellison Medical Foundation (AG-NS-0324-06), the National Institutes of Neurological Disease and Stroke (R01NS059876-03) and the National Cancer Institute (P50CA127001-02).

Grant Support: (i) NIH/NINDS R01NS059876-03, (ii) Ellison Medical Foundation AG-NS-0324-06, and (iii) NIH/NCI P50CA127001

References

1. Gilbertson RJ, Gutmann DH. Tumorigenesis in the brain: location, location, location. Cancer Res. 2007; 67:5579–82. [PubMed: 17575119]
2. Brem SS, Bierman PJ, Brem H, Butowski N, Chamberlain MC, Chiocca EA, et al. Central nervous system cancers. J Natl Compr Canc Netw. 2011; 9:352–400. [PubMed: 21464144]
3. Furnari FB, Fenton T, Bachoo RM, Mukasa A, Stommel JM, Stegh A, et al. Malignant astrocytic glioma: genetics, biology, and paths to treatment. Genes Dev. 2007; 21:2683–710. [PubMed: 17974913]
4. Ohgaki H. Genetic pathways to glioblastomas. Neuropathology. 2005; 25:1–7. [PubMed: 15822813]
5. Louis DN. Molecular pathology of malignant gliomas. Annu Rev Pathol. 2006; 1:97–117. [PubMed: 18039109]
6. Gilbertson RJ, Rich JN. Making a tumour's bed: glioblastoma stem cells and the vascular niche. Nat Rev Cancer. 2007; 7:733–6. [PubMed: 17882276]
7. Drappatz J, Norden AD, Wen PY. Therapeutic strategies for inhibiting invasion in glioblastoma. Expert Rev Neurother. 2009; 9:519–34. [PubMed: 19344303]
8. Hoelzinger DB, Demuth T, Berens ME. Autocrine factors that sustain glioma invasion and paracrine biology in the brain microenvironment. J Natl Cancer Inst. 2007; 99:1583–93. [PubMed: 17971532]
9. Lucio-Eterovic AK, Piao Y, de Groot JF. Mediators of glioblastoma resistance and invasion during antivascular endothelial growth factor therapy. Clin Cancer Res. 2009; 15:4589–99. [PubMed: 19567589]
10. Paez-Ribes M, Allen E, Hudock J, Takeda T, Okuyama H, Vinals F, et al. Antiangiogenic therapy elicits malignant progression of tumors to increased local invasion and distant metastasis. Cancer Cell. 2009; 15:220–31. [PubMed: 19249680]
11. Hynes RO. Integrins: bidirectional, allosteric signaling machines. Cell. 2002; 110:673–87. [PubMed: 12297042]
12. Hynes RO, Lively JC, McCarty JH, Taverna D, Francis SE, Hodivala-Dilke K, et al. The diverse roles of integrins and their ligands in angiogenesis. Cold Spring Harb Symp Quant Biol. 2002; 67:143–53. [PubMed: 12858535]
13. McCarty JH, Monahan-Earley RA, Brown LF, Keller M, Gerhardt H, Rubin K, et al. Defective associations between blood vessels and brain parenchyma lead to cerebral hemorrhage in mice lacking alphav integrins. Mol Cell Biol. 2002; 22:7667–77. [PubMed: 12370313]
14. Zhu J, Motejlek K, Wang D, Zang K, Schmidt A, Reichardt LF. beta8 integrins are required for vascular morphogenesis in mouse embryos. Development. 2002; 129:2891–903. [PubMed: 12050137]
15. McCarty JH, Lacy-Hulbert A, Charest A, Bronson RT, Crowley D, Housman D, et al. Selective ablation of alphav integrins in the central nervous system leads to cerebral hemorrhage, seizures, axonal degeneration and premature death. Development. 2005; 132:165–76. [PubMed: 15576410]
16. Proctor JM, Zang K, Wang D, Wang R, Reichardt LF. Vascular development of the brain requires beta8 integrin expression in the neuroepithelium. J Neurosci. 2005; 25:9940–8. [PubMed: 16251442]
17. Mu D, Cambier S, Fjellbirkeland L, Baron JL, Munger JS, Kawakatsu H, et al. The integrin alpha(v)beta8 mediates epithelial homeostasis through MT1-MMP-dependent activation of TGF-beta1. J Cell Biol. 2002; 157:493–507. [PubMed: 11970960]
18. Mu Z, Yang Z, Yu D, Zhao Z, Munger JS. TGFbeta1 and TGFbeta3 are partially redundant effectors in brain vascular morphogenesis. Mech Dev. 2008; 125:508–16. [PubMed: 18343643]
19. Mobley AK, Tchaicha JH, Shin J, Hossain MG, McCarty JH. {beta}8 integrin regulates neurogenesis and neurovascular homeostasis in the adult brain. J Cell Sci. 2009; 122:1842–51. [PubMed: 19461074]

20. Mobley AK, McCarty JH. beta8 integrin is essential for neuroblast migration in the rostral migratory stream. Glia. 2011
21. Su H, Kim H, Pawlikowska L, Kitamura H, Shen F, Cambier S, et al. Reduced expression of integrin alphavbeta8 is associated with brain arteriovenous malformation pathogenesis. Am J Pathol. 2010; 176:1018–27. [PubMed: 20019187]
22. Tchaicha JH, Mobley AK, Hossain MG, Aldape KD, McCarty JH. A mosaic mouse model of astrocytoma identifies alphavbeta8 integrin as a negative regulator of tumor angiogenesis. Oncogene. 2010; 29:4460–72. [PubMed: 20531304]
23. Sonoda Y, Ozawa T, Hirose Y, Aldape K, McMahon M, Berger MS, et al. Formation of intracranial tumors by genetically modified human astrocytes defines four pathways critical in the development of human anaplastic astrocytoma. Cancer Res. 2001; 61:4956–60. [PubMed: 11431323]
24. Jung Y, Kissil JL, McCarty JH. beta8 integrin and band 4.1B cooperatively regulate morphogenesis of the embryonic heart. Dev Dyn. 2011; 240:271–7. [PubMed: 21181944]
25. McCarty JH, Cook AA, Hynes RO. An interaction between {alpha}v{beta}8 integrin and Band 4.1B via a highly conserved region of the Band 4.1 C-terminal domain. Proc Natl Acad Sci U S A. 2005; 102:13479–83. [PubMed: 16157875]
26. Kissler S, Stern P, Takahashi K, Hunter K, Peterson LB, Wicker LS. In vivo RNA interference demonstrates a role for Nramp1 in modifying susceptibility to type 1 diabetes. Nat Genet. 2006; 38:479–83. [PubMed: 16550170]
27. Abe M, Harpel JG, Metz CN, Nunes I, Loskutoff DJ, Rifkin DB. An assay for transforming growth factor-beta using cells transfected with a plasminogen activator inhibitor-1 promoter-luciferase construct. Anal Biochem. 1994; 216:276–84. [PubMed: 8179182]
28. Ellegala DB, Leong-Poi H, Carpenter JE, Klibanov AL, Kaul S, Shaffrey ME, et al. Imaging tumor angiogenesis with contrast ultrasound and microbubbles targeted to alpha(v)beta3. Circulation. 2003; 108:336–41. [PubMed: 12835208]
29. Erdreich-Epstein A, Shimada H, Groshen S, Liu M, Metelitsa LS, Kim KS, et al. Integrins alpha(v)beta3 and alpha(v)beta5 are expressed by endothelium of high-risk neuroblastoma and their inhibition is associated with increased endogenous ceramide. Cancer Res. 2000; 60:712–21. [PubMed: 10676658]
30. Riemenschneider MJ, Mueller W, Betensky RA, Mohapatra G, Louis DN. In situ analysis of integrin and growth factor receptor signaling pathways in human glioblastomas suggests overlapping relationships with focal adhesion kinase activation. Am J Pathol. 2005; 167:1379–87. [PubMed: 16251422]
31. Bachoo RM, Maher EA, Ligon KL, Sharpless NE, Chan SS, You MJ, et al. Epidermal growth factor receptor and Ink4a/Arf: convergent mechanisms governing terminal differentiation and transformation along the neural stem cell to astrocyte axis. Cancer Cell. 2002; 1:269–77. [PubMed: 12086863]
32. Uhrbom L, Dai C, Celestino JC, Rosenblum MK, Fuller GN, Holland EC. Ink4a-Arf loss cooperates with KRas activation in astrocytes and neural progenitors to generate glioblastomas of various morphologies depending on activated Akt. Cancer Res. 2002; 62:5551–8. [PubMed: 12359767]
33. Holland EC, Celestino J, Dai C, Schaefer L, Sawaya RE, Fuller GN. Combined activation of Ras and Akt in neural progenitors induces glioblastoma formation in mice. Nat Genet. 2000; 25:55–7. [PubMed: 10802656]
34. Hahn WC, Counter CM, Lundberg AS, Beijersbergen RL, Brooks MW, Weinberg RA. Creation of human tumour cells with defined genetic elements. Nature. 1999; 400:464–8. [PubMed: 10440377]
35. Blouw B, Song H, Tihan T, Bosze J, Ferrara N, Gerber HP, et al. The hypoxic response of tumors is dependent on their microenvironment. Cancer Cell. 2003; 4:133–46. [PubMed: 12957288]
36. Cambier S, Gline S, Mu D, Collins R, Araya J, Dolganov G, et al. Integrin alpha(v)beta8-mediated activation of transforming growth factor-beta by perivascular astrocytes: an angiogenic control switch. Am J Pathol. 2005; 166:1883–94. [PubMed: 15920172]

37. Liang CC, Park AY, Guan JL. In vitro scratch assay: a convenient and inexpensive method for analysis of cell migration in vitro. Nat Protoc. 2007; 2:329–33. [PubMed: 17406593]
38. Ozdamar B, Bose R, Barrios-Rodiles M, Wang HR, Zhang Y, Wrana JL. Regulation of the polarity protein Par6 by TGFbeta receptors controls epithelial cell plasticity. Science. 2005; 307:1603–9. [PubMed: 15761148]
39. Wu MY, Hill CS. Tgf-beta superfamily signaling in embryonic development and homeostasis. Dev Cell. 2009; 16:329–43. [PubMed: 19289080]
40. Bruna A, Darken RS, Rojo F, Ocana A, Penuelas S, Arias A, et al. High TGFbeta-Smad activity confers poor prognosis in glioma patients and promotes cell proliferation depending on the methylation of the PDGF-B gene. Cancer Cell. 2007; 11:147–60. [PubMed: 17292826]
41. Penuelas S, Anido J, Prieto-Sanchez RM, Folch G, Barba I, Cuartas I, et al. TGF-beta increases glioma-initiating cell self-renewal through the induction of LIF in human glioblastoma. Cancer Cell. 2009; 15:315–27. [PubMed: 19345330]
42. Seoane J. Escaping from the TGFbeta anti-proliferative control. Carcinogenesis. 2006; 27:2148–56. [PubMed: 16698802]
43. Fang L, Deng Z, Shatseva T, Yang J, Peng C, Du WW, et al. MicroRNA miR-93 promotes tumor growth and angiogenesis by targeting integrin-beta8. Oncogene. 2010; 30:806–21. [PubMed: 20956944]
44. Markovics JA, Araya J, Cambier S, Jablons D, Hill A, Wolters PJ, et al. Transcription of the transforming growth factor beta activating integrin beta8 subunit is regulated by SP3, AP-1, and the p38 pathway. J Biol Chem. 2010; 285:24695–706. [PubMed: 20519498]
45. Cambier S, Mu DZ, O'Connell D, Boylen K, Travis W, Liu WH, et al. A role for the integrin alphavbeta8 in the negative regulation of epithelial cell growth. Cancer Res. 2000; 60:7084–93. [PubMed: 11156415]
46. McCarty JH, Barry M, Crowley D, Bronson RT, Lacy-Hulbert A, Hynes RO. Genetic ablation of alphav integrins in epithelial cells of the eyelid skin and conjunctiva leads to squamous cell carcinoma. Am J Pathol. 2008; 172:1740–7. [PubMed: 18467691]
47. Kanamori M, Vanden Berg SR, Bergers G, Berger MS, Pieper RO. Integrin beta3 overexpression suppresses tumor growth in a human model of gliomagenesis: implications for the role of beta3 overexpression in glioblastoma multiforme. Cancer Res. 2004; 64:2751–8. [PubMed: 15087390]
48. Bello L, Francolini M, Marthyn P, Zhang J, Carroll RS, Nikas DC, et al. Alpha(v)beta3 and alpha(v)beta5 integrin expression in glioma periphery. Neurosurgery. 2001; 49:380–9. discussion 90. [PubMed: 11504114]
49. Treasurywala S, Berens ME. Migration arrest in glioma cells is dependent on the alphav integrin subunit. Glia. 1998; 24:236–43. [PubMed: 9728769]
50. Chatterjee S, Matsumura A, Schradermeier J, Gillespie GY. Human malignant glioma therapy using anti-alpha(v)beta3 integrin agents. J Neurooncol. 2000; 46:135–44. [PubMed: 10894366]
51. Skuli N, Monferran S, Delmas C, Favre G, Bonnet J, Toulas C, et al. Alphavbeta3/alphavbeta5 integrins-FAK-RhoB: a novel pathway for hypoxia regulation in glioblastoma. Cancer Res. 2009; 69:3308–16. [PubMed: 19351861]
52. Shi Q, Hjelmeland AB, Keir ST, Song L, Wickman S, Jackson D, et al. A novel low-molecular weight inhibitor of focal adhesion kinase, TAE226, inhibits glioma growth. Mol Carcinog. 2007; 46:488–96. [PubMed: 17219439]
53. Blouw B, Haase VH, Song H, Bergers G, Johnson RS. Loss of vascular endothelial growth factor expression reduces vascularization, but not growth, of tumors lacking the Von Hippel-Lindau tumor suppressor gene. Oncogene. 2007; 26:4531–40. [PubMed: 17297464]
54. Nakagawa T, Lan HY, Zhu HJ, Kang DH, Schreiner GF, Johnson RJ. Differential regulation of VEGF by TGF-beta and hypoxia in rat proximal tubular cells. Am J Physiol Renal Physiol. 2004; 287:F658–64. [PubMed: 15187003]
55. Sanchez-Elsner T, Botella LM, Velasco B, Corbi A, Attisano L, Bernabeu C. Synergistic cooperation between hypoxia and transforming growth factor-beta pathways on human vascular endothelial growth factor gene expression. J Biol Chem. 2001; 276:38527–35. [PubMed: 11486006]

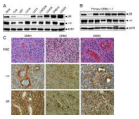

Figure 1. Analysis of β8 integrin protein expression in human GBM cell lines and freshly resected tumor samples

(A); Detergent-soluble lysates from normal human astrocytes (NHAs), transformed human astrocytes (THAs) and 7 different human GBM cell lines were immunoblotted with anti-αv or anti-β8 integrin antibodies. Note that NHAs express robust levels of αv and β8 integrin proteins, with oncogene-induced transformation leading to reduced integrin expression in THAs. In addition, αv and β8 integrin proteins are expressed at varying levels in the different human GBM cell lines. **(B);** Detergent-soluble lysates from 7 different primary GBMs were immunoblotted with anti-αv or anti-β8 integrin antibodies, revealing integrin protein expression in the different samples. **(C);** Formalin fixed paraffin-embedded sections from three different grade IV astrocytomas (GBMs) stained with H&E (top panels), anti-αv integrin antibodies (middle panels), or anti-β8 integrin antibodies (lower panels). Note that αv integrin protein is expressed in GBM cells as well as in intratumoral blood vessels. β8 integrin protein is also expressed in GBM cells, but is largely absent in intratumoral blood vessels. Images are shown at 400x magnification.

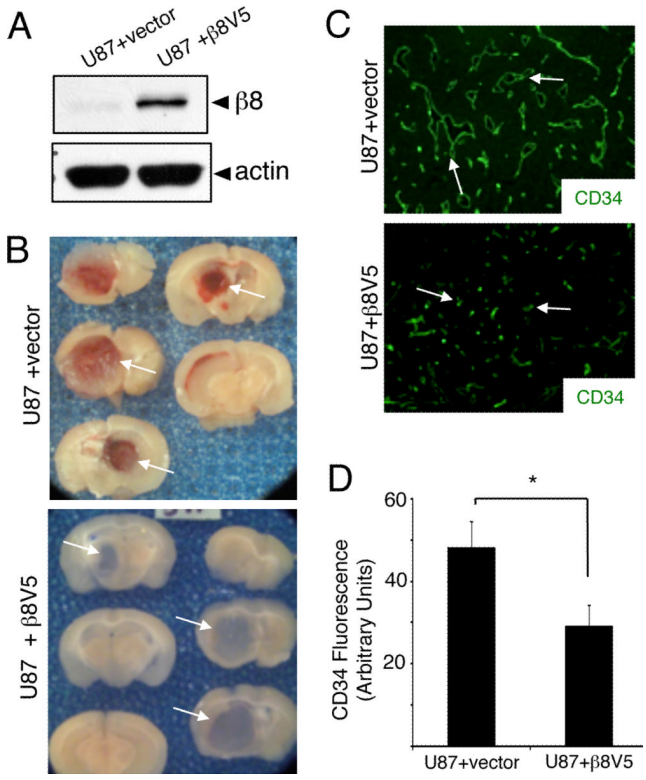

Figure 2. β8 integrin suppresses microvascular pathologies and hemorrhage in GBM

(A); U87 cells were stably transfected with empty plasmid or a plasmid containing a cDNA encoding for a β8-V5 fusion protein. Detergent-soluble lysates were then immunoblotted with antibodies directed against anti-β8 integrin or anti-actin antibodies. Note the increased expression of β8 integrin protein. **(B);** U87 cells stably transfected with empty plasmid (top panels) or plasmid harboring a β8-V5 cDNA (bottom panels) were stereotactically injected into the striatum of immunocompromised mice (n=5 mice per cell type). Shown are gross images of slices from representative brains harboring tumors generated from each cell type. Note that the intratumoral hemorrhage evident in the U87 tumors is not evident in tumors overexpressing β8-V5 protein. **(C);** U87 tumors stably transfected with empty plasmid or plasmid expressing β8-V5 were immunostained with an anti-CD34 antibody to visualize vascular endothelial cells (n=3 different brains per cell type). Note the increased numbers of blood vessels and abnormal morphologies in U87 tumors transfected with empty plasmid versus the capillary-like morphologies in U87 tumors overexpressing β8 integrin. **(D);** Immunofluorescence intensities were quantified based on anti-CD34 antibody staining (shown at 200x magnification). Note the significant reduction of fluorescent intensity in U87 tumors forcibly expressing β8-V5 integrin protein (*$p<0.0001$). Error bars represent standard deviations.

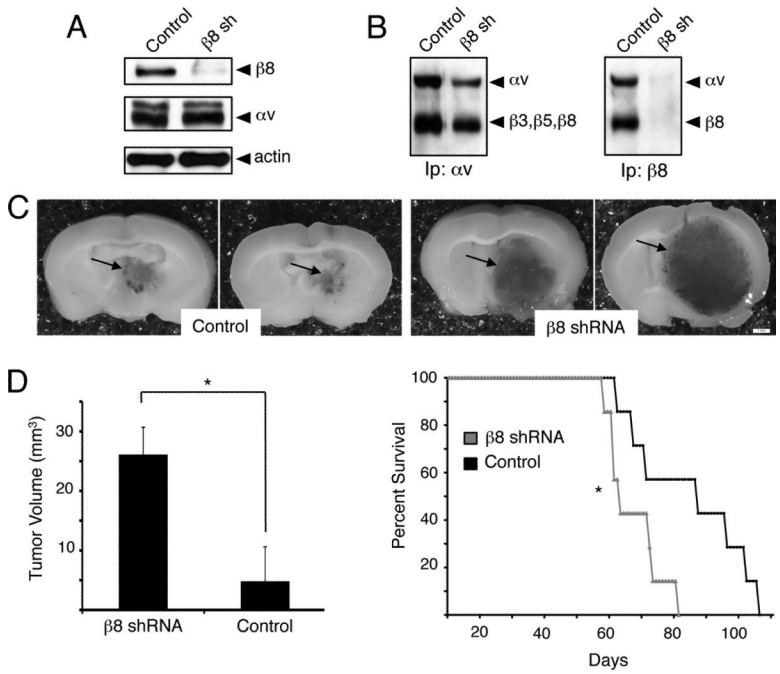

Figure 3. Silencing β8 integrin expression in transformed human astrocytes leads to enhanced tumor growth

(A); THAs were transduced with pLB lentivirus expressing non-targeting scrambled shRNAs (control) or shRNAs targeting human β8 integrin (β8 shRNA). Detergent-soluble lysates were immunoblotted with anti-integrin antibodies, revealing a significant reduction in β8 integrin protein expression. **(B);** THAs were incubated with an amine-reactive biotin to label cell surface proteins. Detergent-soluble lysates were then immunoprecipitated with anti-αv or anti-β8 integrin antibodies. THAs expressing control and β8 shRNAs contain robust levels of αv-containing integrins on their cell surfaces (left panel). In contrast, note the low levels of cell surface-expressed αvβ8 integrin protein in THAs expressing β8 shRNAs (right panel). **(C);** NCR-nu/nu mice (n=8 per cell type) were stereotactically injected with THAs expressing β8 shRNAs (right panels) or scrambled shRNAs (left panels). Shown are images of two representative brains containing astrocytomas. Tumors generated from THAs expressing β8 shRNAs are larger and display severe hemorrhage (arrows). **(D);** Significantly larger astrocytoma volumes, as determined by measuring cross-sectional areas of H&E-stained tumors expressing β8 shRNAs versus scrambled shRNAs (left graph). Kaplan-Meier analysis reveals that mice harboring tumors generated from THAs expressing β8 shRNAs die earlier than animals harboring tumors generated from THAs expressing control shRNAs (right graph), *$p<0.05$. The mean survival times for mice bearing tumors derived from control THAs is 84 days, whereas the mean survival for mice harboring tumors derived from THAs expressing β8 shRNAs is 62 days.

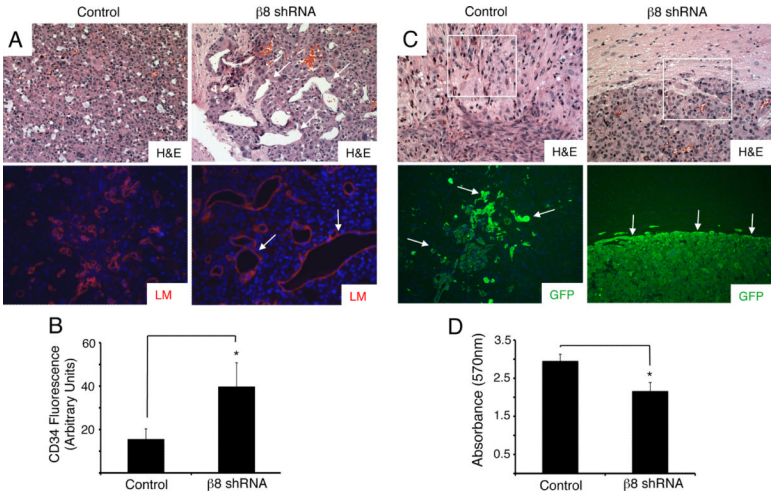

Figure 4. Microscopic analysis of integrin-dependent tumor-induced angiogenesis and tumor cell invasiveness

(A); Coronal sections from control (left, upper panel) and β8 shRNA (right, upper panel) astrocytomas were stained with H&E. Sections were also immunolabeled with an antibody directed against laminin (lower panels). Note the enlarged blood vessel sizes and abnormal morphologies in tumors derived from THAs expressing β8 shRNAs (arrows in right panel). Images are shown at 200x magnification. **(B);** Coronal sections from control or β8 shRNA astrocytomas (n=3 tumors per cell type, n=5 sections per tumor) were immunostained with anti-CD34 to visualize vascular endothelial cells and fluorescence intensities were quantified, *p<0.001. Error bars represent standard deviations. **(C);** H&E-stained coronal sections from astrocytomas generated from THAs expressing control shRNAs (left, upper panel) or shRNAs targeting β8 integrin (right, upper panel). Coronal sections from control (left, lower panel) and β8 shRNA tumors (right, lower panel) were immunofluorescently labeled with an antibody directed against GFP, revealing robust expression in tumor cells. Note the well-defined and non-invasive tumor peripheries in β8 shRNA samples (arrows in right lower panel) as compared to the infiltrative tumors cells in control astrocytomas (arrows in left lower panel). Images are shown at 200x magnification. **(D);** THAs expressing β8 shRNAs showed a significant reduction in invasiveness through three-dimensional extracellular matrices as compared to THAs expressing scrambled shRNAs. Triplicate samples were analyzed for each cell type, *p<0.001. Error bars represent standard deviations.

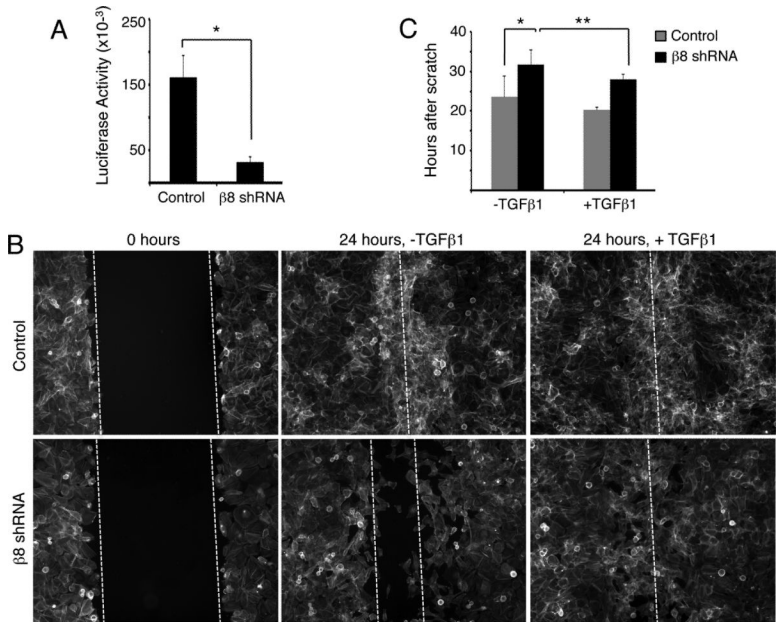

Figure 5. Integrin-activated TGFβs promote astrocytoma cell migration

(A); THAs expressing scrambled shRNAs or β8 shRNAs were transiently transfected with a PAI1-Luciferase (PAI1-L) plasmid to measure TGFβ signaling. Triplicate samples were analyzed for each cell type, *p<0.001. Error bars represent standard deviation. **(B);** Confluent monolayers of control or β8 shRNA THAs were scratched and 24 hours later cells were labeled with phalloidin-FITC. Note that THAs expressing scrambled shRNAs fill the wound area within 24 hours, whereas THAs expressing β8 shRNAs show diminished migration. Exogenous addition of TGFβ1 significantly enhanced THA directional migration. Double dashed lines indicate wound boundaries and single dashed white lines indicate closed wounds. Images are shown at 100x magnification. **(C);** Quantification of integrin-dependent cell migration. Confluent monolayers of THAs expressing scrambled or β8 shRNAs were scratched and migration was imaged over 48 hours using time-lapse microscopy (n=3 different samples per cell type). THAs expressing scrambled shRNAs (grey bars) filled the wound area within 24 hours, whereas THAs expressing β8 shRNAs (black bars) show diminished migration and required nearly 36 hours to fill the wound region. Exogenous addition of TGFβ1 significantly enhanced THA directional migration, *p=0.006 and **p=0.03. The migration rates between control cells with or without TGFβ1 are not statistically significant. Error bars represent standard deviations.

Figure 6. A model for β8 integrin-mediated regulation of GBM angiogenesis versus tumor cell invasiveness

(A); In the normal brain astrocytes and neural progenitor cells (NP) express αvβ8 integrin and regulate cerebral blood vessel (BV) development and physiology via activation of TGFβ signaling pathways. **(B);** Genetic mutations in NPs induce their transformation and initiate development of astrocytomas that maintain αvβ8 integrin expression. **(C, D);** As astrocytomas progress to GBM, sub-populations of tumor cells express different levels of αvβ8 integrin protein. Cells with low αvβ8 integrin protein ($\alpha v\beta 8^{lo}$) activate diminished levels of TGFβs and contribute to angiogenesis and vascular permeability pathologies (C). In contrast, cells that express elevated levels of αvβ8 integrin protein ($\alpha v\beta 8^{hi}$) activate more TGFβs and drive invasive GBM growth properties (D). Differential levels of integrin-mediated TGFβ activation and signaling likely cooperate with the Hif1α/VEGF-A pathway to regulate angiogenesis versus tumor cell invasiveness.